International Journal for Innovation Education and Research
scholarsjournal.net/index.php/ijier ISSN: 2411-2933

DOI: doi.org/10.31686/ijier.vol10.iss8.3854

Application of a Logit Model for Water well site location in fractured-bedrock aquifers in northeastern Brazil

Yesus Emmanuel Medeiros Vieira, Renata Albergaria de Mello Bandeira, Orivalde Soares da Silva Junior

Abstract

Wells drilling process in fractured-bedrock aquifers is a difficult task. Extreme variations in lithology and structure features, as well productive water zones sited at preferential points make geological and geophysical investigations difficult. To contribute to the understanding of the process of groundwater zones occurrence in fractured-bedrock aquifers, this paper develops a drilling prospective model by using regression analysis, whose parameters were calibrated according to the photogeological and cartographic analysis of 113 drilling points in the states of Rio Grande do Norte, Paraíba, and Ceará. The effectiveness of the resulting model was assessed through a sample of 43 additional drillings, which were carried out aiming at the distribution of water to the communities in the semiarid region of Brazil. The obtained results indicate the model as an important tool in the drilling process, with direct implications on the logistics costs of water well site location and consequent attendance to the population that needs the water.

Keywords: Fractured-bedrock aquifer; Remote sensing; Groundwater favorability map.

1. INTRODUCTION

Drought is one of the costliest natural disasters, resulting in disastrous impacts on society and ecosystems, such as, for ex-ample, the incident in US in 2012 and the drought in East Africa 2010/2011, leading to substantial and hungry economic econo-mies worldwide (Hao et al., 2017). Drought is defined as a re-curring weather phenomenon that results from the reduction of rainfall, gradually letting the water insufficient to meet the needs of humans and ecosystems (Ortega-Gaucin; López Pérez; Ar-reguín, 2016). For these reasons, it is essential that regional leaders and managers who propose drought determine threats and innovations for drought risk mitigation and preparedness (Nam et al. 2015).

In Brazil, this phenomenon mainly affects the semiarid northeas-tern region of the country, which concentrates most of Brazil's poorest population - approximately 28 million people (Cunha et al. 2019). Groundwater accounts for only 20% of the world's fresh water supply, representing only 0.61% of the world's wa-ter, including oceans and permanent ice (Adetoyinbo; adelegan; bello, 2015). In drought regions with hydrogeological characte-ristics as those observed northeastern Brazil the groundwater occurs in watersheds within hard rock aquifers and is controlled mainly due to secondary porosity caused by the underlying rock fracture (Nag, 2016; Singh et al., 2019). Additionally, factors such as terrain slope, geomorphology, lithology, precipitation, topo-graphic elevation, drainage, land use /land cover, and lineament often provide an indication of groundwater location (Abuzied; Alrefaee, 2017). Given these circumstances, groundwater pros-pecting without proper hydrogeological surveys often leads to failures due to the complex geological structure and irregular nature of these water resources in crystalline rock environ-ments (Sivaramakrishnan et al. 2015).

For these reasons, the use of technologies that integrate con-ventional methods with modern techniques of remote sensing and geographic information system (GIS) has been helping to increase the accuracy of hydrogeological research results, as well as to delineate potential groundwater zones in this type of region (Das, 2017). In turn, the use of geophysics in aquifer mapping and water quality assessment has also grown, due in large part to the positive results achieved, which are associated with advances in numerical modeling solutions (Sa; Elis, 2016; Redhaounia et al., 2016). Among the geophysical techniques that can assist in the identification of artesian wells in fractured aqui-fers, the multi-electrode resistivity method is one of the most widely used in geological studies. (hydrogeology, mapping, mi-ning), civil engineering and environmental studies in general, offering advantages in terms of speed, low cost and satisfactory results in mineral exploration (Silva et al., 2018).

Several recent studies have employed remote sensing tech-niques and GIS, sometimes combined with geophysical methods, in order to define prospective groundwater zones in fissural aquifers (Binley et al. (2015); Mohamaden et al., 2017; Abuzied et al, 2016; Nazuridin et al., 2017; Abuzied; Alrefaee, 2017; Aziz; Hasan; Abdulrazzaq 2018). However, studies adopting these approaches remain scarce in the Brazilian scenario (Brandão; Gomes, 2003; Madrucci; Taioli; De Araújo, 2008; Elis et al., 2019), despite the relevance and economic and social impacts of drought in the Brazilian scenario. The analyzes carried out in Brazil, in general, are insufficiently conducted in the northeast region, do not allowing a better analyze of variations of the factors that usually influence the prediction of groundwater occurrence, given the limited territorial extensions in which the experiments were performed. Thus, a larger-scale analysis of these prediction constraints, especially in the case of numerous and dispersed drilling in hydro geologically varied environments, such as those carried out by government programs in the semi-arid region of northeastern Brazil, is an important tool in the well drilling process, implicating on the logistics cost of this activity and the amount of productive wells delivered to the population in need of water.

Thus, this paper aims to propose a prediction model for the of potential groundwater occurrence zones, in support of the location and drilling activities performed by the Brazilian Army, using the combination of geological survey and multi-electrode resistivity geophysicist method. Due to the inherent complexity of the fractured aquifer, statistical analysis of the hydrogeological characteristics of 113 locations where artesian wells were dril-led by the Army in the states of Rio Grande do Norte, Paraíba and Ceará was performed. The prospective model was deve-loped based on the binomial logistic regression statistical tech-nique, which considered the independent variables resulting from the geoprocessing of explanatory factors that theoretically may influence the process of water circulation and storage in fissural media. The effectiveness of the prospective model obtai-ned was evaluated through a sample of 43 additional perfora-tions, performed aiming at the distribution of water to the communities served by a response plan, called

"Operação Carro Pipa" (operation that takes water for human consumption in areas affected by drought in the Northeast region) (Cunha et al. 2019). Improvements in successful drilling rates in these locations have an impact not only on the government costs involved in prospecting activities but also have a direct social implication on life quality of the population in need of water.

This paper is structured as follows: a brief description of the study area and geological context are presented in Section 1. Section 2 describes the methodology adopted in the logistic regression model generation and field trials. Section 3 presents the research results are presented, analyzed and discussed. Finally, Section 4 presents the conclusions, research limitations, and suggestions for future work.

2. MATERIALS AND METHODS

2.1 Study Area.

The Brazilian Army, in partnership with the Ministry of National Integration, has been drilling boreholes in Minas Gerais and seven Northeastern states. This operation has begun in May 2016, for at 16 million BRL, and has provided for the drilling of 500 artesian wells to increase water availability and water security of the Brazilian semiarid population (Brazilian Army, 2018).

Figure 1 presents the geographical distribution of artesian wells analyzed in this paper (blue dots). The wells are inserted in the geological context of the province of Borborema, encom-passing the Domínio Ceará Central (DCC), Domínio Jaguaribeano (DJ) and Domínio Rio Piranhas-Seridó (DPS), occupying an extensive area in the south-central part of the state of Rio Grande do Norte, Ceará and Paraíba, and including several lithologies.

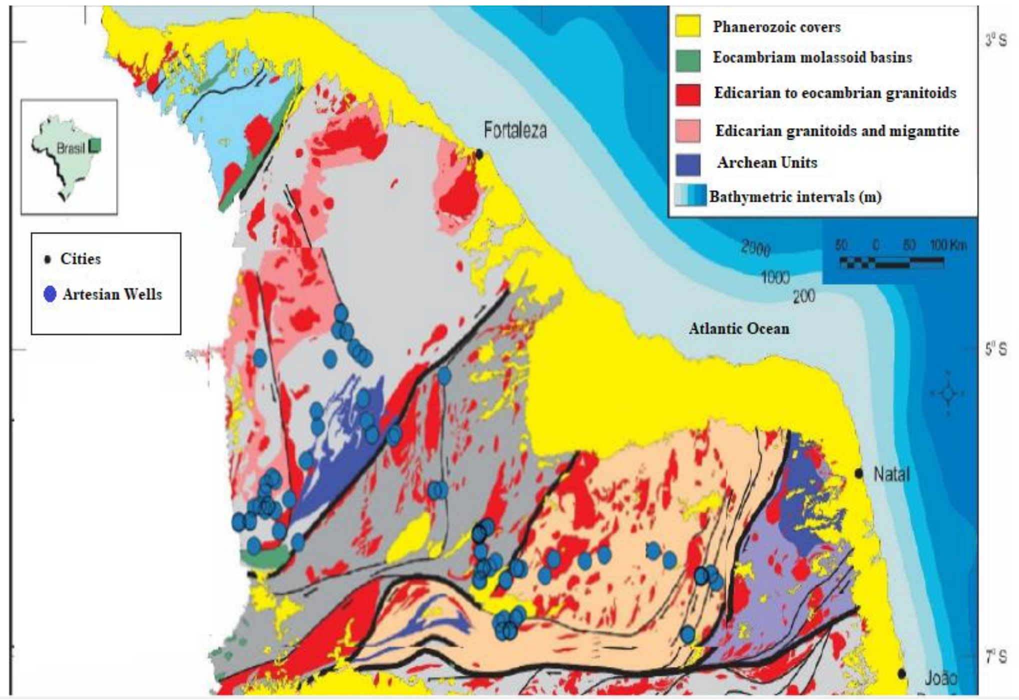

Figure 1 . Localization of Domínio Piranhas-Seridó (DPS) in the context of Borborema Province.
Source: adapted from Medeiros et al. (2005).

Among the main challenges involved in wells drilling, it is highlighted the definition of adequate places for wells drilling in regions of fractured-bedrock aquifers. This activity demands constant scientifically and technologically efforts to improve the current approaches and construction techniques. The Brazilian Army's groundwater prospecting at these sites still lacks techni-cal and scientific grounding, reflecting on a large number of un-productive wells and requiring studies focusing on more efficient models to subsidize the selection of favorable areas for drilling of artesian wells.

The cases studied in this paper are associated with fractured-bedrock aquifers, where, according to Feitosa (2008), ground-water occurs in interconnected, discontinuous and limited length crack systems and fractures.

2.2 Cartographic data and applied geoprocessing techniques

The definition of the drilling areas studied in this paper was conducted by using photogeological and cartographic analysis, associated with the structural orientations, terrain slope, and water recharge areas. Initially, the principal explanatory variables that theoretically may influence the process of water circulation and storage in fractured-bedrock aquifers were obtained from the related literature (Abuzied; Alrefaee 2017; Feitosa, 2008; Madrucci; Taioli; De Araújo, 2008; Brandão; Gomes, 2003; Gup-ta; 2003). From this review, it was elected for this work the aspects related to subsurface lithology, terrain slope, surface drainage densities, and local and regional structural lineaments, as well as the distance from the drilling points. to structural elements. The cartographic bases used are the geophysical geo-logical integration charts of the corporate database (Geobank) of CPRM (Geological Survey of Brazil) and the hypsometric data contained in the INPE database (2018). Figure 2 presents an illustrative scheme of the evaluated aspects, for the case of Folha CAICÓ (SB.24-Z-B-I), scale 1: 100,000. It is shown in the Figure 2.

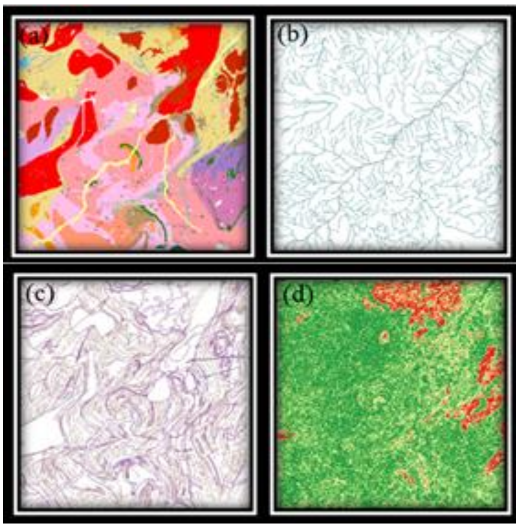

Figure 2. Illustrative scheme of the independent variables evaluated. (a): predominant lithotypes; (b): Surface drainage; (c): Structural lineaments; (d): Slope Source: Prepared by the author.

In order to identify the parameters presented in Figure 2, the cartographic bases used were the geophysical geological integra-tion charts of the CPRM (Geological Service of Brazil) corporate database (Geobank) and the hypsometric data contained in the INPE database (2019). Among the remote sensing products employed in the study, the information obtained from Shuttle Radar Topography Mission (SRTM), available at the National Aeronautics and Space Administration (NASA) website, has a spatial resolution of 30 meters (NASA, 2019).

Thus, with the cartographic representations and the remote sensing products, thematic maps and shaded models were elabo-rated with the aid of the QGIS geoprocessing software (Version 2.8.9) that helped in the extraction and vectorization of the geomorphological features present in the area. study.

The extraction of the superficial drainage segments was obtained automatically, with the aid of the TauDEM (Terrain Analysis Using Digital Elevation Models) tool, that is enabled in the QGIS software environment, and by visual interpretation, in order to obtain a better detailing of these features. The morphometric data were obtained through the field calculator tool of the QGIS software.

The extraction of structural lineaments was performed automa-tically and manually. For automatic extraction, PCI Geomatics V13.0 software was used in the Focus module, using the LINE algorithm (Tools> Algarithm Librarian> LINE: Lineament Extra-tion). This procedure allowed the linear features contained in the images obtained from the remote sensing to be transformed into vector segments by using predefined global parameters or changed according to the user's need. The values used for the LINE algorithm input parameters were those described in the studies by Conceição e Silva (2013) and Silva and Maia (2017), and the basis for the extraction of lineaments in PCI Geomatics was obtained from the shaded and SRTM elevation model, geo-processed by using the QGIS. In this software, in the item Inso-lation azimuth, the angular position of the sun was inserted for different azimuthal directions (45º, 90º, 315º and 360º), and has been adopted for this paper the value 315 °. Another consi-dered parameter was the insolation altitude, which is the inclina-tion of the sun, in degrees, from the horizon, from 0 ° to 90 °, and the standard value used was 45 °. The parameters tested were proposed by Conceição e Silva (2013), considering the number of linear features, the positive and negative behaviors of these features and the preferred directions of the regional li-neaments. The quality evaluation of the automatically extracted lineaments was performed visually in the QGIS software, to obtain a product suitable to the structural reality of the area by positioning the features on the SRTM image in false color and pre-existing morpho-structural maps for the Northeast region.

The geometric characteristics of drainage density (km / km²) and structural elements (km / km²) were extracted using the ArcMap program's LineDensity tool. This allowed the density of linear shapes to be calculated in the vicinity of each cell (pixel) of the output raster. Density is calculated in units of length per unit area (km / km2). Conceptually, this calculation is structured as follows: A circle is drawn around each cell of the image, using as a radius a value arbitrated by the user. The length portion of each feature contained in the circular area is summed and the total is divided by the area of the circle (Figure 3).

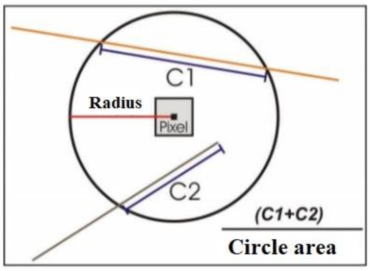

Figure 3. linear density calculation concept, where C1 and C2 are as parts of the length of the lineaments inserted in the circle area. Source: Modified from ESRI, 2019.

2.3 Formulation of a prospective model

The explanatory variables mentioned in the previous sub-item were subdivided into classes, according to their favorable groundwater occurrence aspects (Table 1). Thus, the predomi-nant lithotypes are classified according to the scale presented in Feitosa (2008), while the structural and surface drainage densi-ties were divided into five ordinal classes, with weights ranging from 1 (one) to 9 (nine), following the one proposed by Abuzied and Alrefaee (2017), and adapting the numerical class intervals according to the average values of lineament densities and sur-face drainage identified in the drilling areas of the 113 wells. The slope categories of the land corresponding to the classification established by EMBRAPA (1979).

Additionally, it was decided to verify the influence that the proximity of the drilling point to the geological contacts and structural lineaments has on well productivity. For this purpose, with the aid of QGIS, a circular buffer of 100 meters radius was established, reducing the distance analyzed in Madrucci, Taioli and De Araújo (2008) for crystalline aquifers in the state of São Paulo (250 meters). This modification was adopted taking into account the lower rainfall rates found in the northeast region and the resulting implications for groundwater accumulation in fissural aquifers, as well as to cover the range of the resistivime-ter apparatus used in geophysical surveys.

Table 1– Ranks of thematic layers and weights of their classes based on their relative impacts on groundwater accumulation.

Criteria	Classes	Description/intervals	Groundwater potentiality	Weight
Lithology	1	Undeformed granitoids / quartz diorites / granodiorites / granite tabular	Very poor	3
	2	Paragnaisse / gneissified porphyritic granodiorites and granites	Poor	4
	3	Strongly banded orthognaisses /	Moderate	5

		paraderivated / calcysilicate migmatites		
	4	Shales / quartzites / biotite gneisses / metacalcary	Good	6
	5	Alluvium	Very good	9
Lineament density (Km/Km²)	1	0-0,490|	Very poor	1
	2	0,490-0,980|	Poor	3
	3	0,980-1,470|	Moderate	5
	4	1,470-1,960|	Good	7
	5	>1,960	Very good	9
Drainage density (Km/Km²)	1	0-0,452|	Very poor	1
	2	0,452-0,904|	Poor	3
	3	0,904-1,356|	Moderate	5
	4	1,356-1,808|	Good	7
	5	>1,808	Very good	9
Terrain slope	1	0-2%| plain	Very poor	1
	2	2%-5%| Smooth wavy	Poor	3
	3	5%-10%| Ondulado	Moderate	5
	4	10%,-15%| Moderately wavy	Good	7
	5	15%-45%| Tightly wavy	Very good	9
Distance from candidate drilling point to nearest lineament	1	<100m	Favourable	1
	2	>100m	Unfavourable	0

After identification the corresponding values of the four explanatory variables listed for each to the 113 wells under study, these factors were submitted to the chi-square and correlation statistical tests, to confirm which variables did influence the productivity. of the analyzed wells. After this step, the prospective model was developed in the form of logistic regression, following the mathematical expression presented in Equation 1, as follows:

$$f(z) = \left(\frac{1}{1+e^{-z}}\right) \qquad (1)$$

where f (z) is defined as the probability of occurrence of the event, which, for the present article, will be defined as the probability of drilling a well with a flow rate greater than $1m^3$ / h. The function z is defined as $z = \beta_0 + \beta_1 X_{i1} + \beta_2 X_{i2} + \cdots + \beta_k X_{ik}$, where β_0 is the intercept and $\beta_1, \beta_2 \ldots, \beta_k$ are the parameters of the regression model, where k is the number of attributes of the alternatives, and $X_{i1}, X_{i2} \ldots, X_{ik}$ represent the values of the attributes of the independent variables, presented in Table 1.

The obtained model was validated by drilling additional wells. The sample size calculation followed Equation (2), obtained from Zar (1999), which allows comparing performances between two different location techniques.

$$n = \frac{\left[z_\alpha\sqrt{2P_0Q_0} + w_\beta\sqrt{P_AQ_A + P_BQ_B}\right]^2}{(P_A - P_B)^2} \qquad (2)$$

wherein:

n= sample size;

z_α= critical z value for a bilateral test with a significance level of α;

w_β= critical z value for a one-sided test for a type II error probability equal to β;

P_A= supposedly true proportion of productive wells obtained by exclusively with field location techniques - Method A.

P_B= supposedly true proportion of productive wells obtained by using GIS tools and geophysical techniques: - Method B.

$$P_0 = \frac{(P_A + P_B)}{2}$$

$$Q_0 = 1 - P_0$$

$$Q_A = 1 - P_A$$

$$Q_B = 1 - P_B$$

For the application of Equation (2), this work adopted the index P_A de 41% corresponding to the drilling of the successful well adopting field location techniques, according to results obtained in the last 113 drillings conducted by the Brazilian Army, and the P_B index of 75% success through the conventional method combined with the geophysical one, observed average value of recent studies published in fractured-bedrock aquifers in Brazil (Gallas and Giardin, 2016; Silva; Rodrigues; Lisboa, 2018; Sá and Elis, 2016).

The wells were drilled using a Prominas model R-1S drill. This equipment is able to drilling wells up to 250 meters deep. In drilling, 10.1 / 2 "or 9.7 / 8" diameter bits were used in the initial well phase. In the intermediate phase of drilling, 8 "drill and 6" in diameter were used.

2.4 Geophysical techniques

The geophysical surveys were conducted by multi-electrode resistivity method. For geophysical investigations, this method is usually adopted in groundwater prospecting because it satisfies the basic condition for identification of an aquifer, which is the presence of contrast between the quantities, delimiting, for example, the zones of fractures saturated in water, vertically and horizontally (Giampá and Gonçales, 2009). The method is based on the measurement of the intensity of a physical quantity present in the material, called electrical resistivity (ρ), which varies according to its mineralogical or chemical composition, particle size, saturation, compaction, cementation among other aspects (Keary et al., 2009). The electrical resistivity can be explained according to the equation: ρ a = K.ΔV / I mm, where (I) is the intensity of the current running through the subsurface, (K) the geometry of the electrode array, and (ΔV) a potential difference measured by the receiving electrodes. It is possible to calculate the apparent resistivity value due to heterogeneity. The unit of apparent resistivity is measured in Ohm.m, the potential difference is measured in millivolt (mV), while the current intensity is measured in milliampere (mA) and the geometric coefficient K in meters.

The electrode array used in this work was the Dipole-Dipole (D-D), since it presents acceptable resolution and at the same time a high data acquisition speed (Martonara et al., 2017), as illustrated in Figure 4.

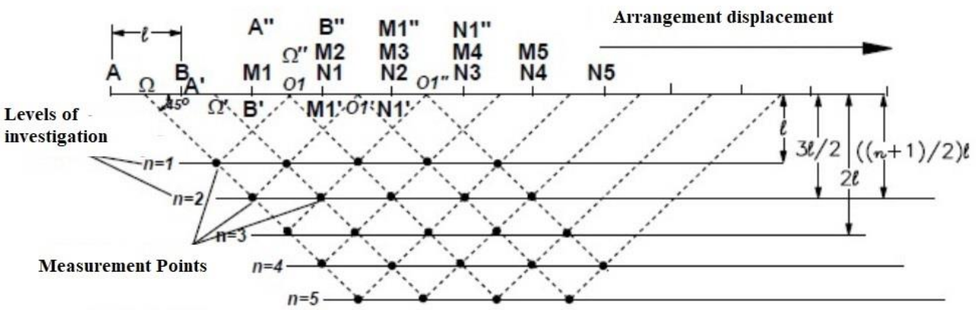

Figure 4 – Dipole-Dipole (D-D) configuration used in this study.

The experiments performed with D-D arrangement were conducted by using Supersting R8 equipment, containing 8 channels, 84 electrodes and 200W power were used. Each survey presented specific electrode spacing and line length configurations, due to the physical space limitations found at the sites, providing theoretical depths of investigation up to 70 to 110 meters deep.

Apparent resistivity data were measured and processed by using RES2DINV software, an inversion program for electric resistivity data that supports two inversion algorithms (robust and smoothness), terrain topography data, and user-friendly graphical interface. The method adopted for data inversion was the robust inversion method (Oldenburg; Li, 1999). In the case of an irregular morphology, topographic correction was applied based on the topographic data collected successively to the geophysical surveys.

3. RESULTS AND DISCUSSIONS

The flow rates of the studied wells were categorized into two productivity classes, according to the division established in Feitosa (2008). To confirm whether there is a relationship between the productivity classes of the 113 wells drilled and the decision variables described in Table 1, Chi-square and Spearman correlation tests were performed.

For the chi-square test, at a significance level of 5%, it was observed that the slope of the terrain did not exert statistical significance on the variation in productivity of the wells since almost all of them were located in flat areas or smoothly wavy. In turn, it was found that the variation in the production class of drilled wells is influenced by the decision variables predominant lithotype, drainage density and density of structural lineaments and distance from the well to geological contact, according to Table 2.

Table 2. Chi-square statistics of predictive variables of groundwater occurrence.

	Lithology	**Drainage density**	**Lineament density**	**Slope**	**Distance from candidate drilling point to nearest lineament**
Qui-quadrado	8,318	5,845	5,018	2,820	26,21
gl	1	1	1	1	1
Significância	0,004	0,016	0,025	0,43	0,000

Spearman's test indicated positive correlations between wells flow rate classes and three independent variables (lithology, lineament density, and surface drainage density) (Table 3). These positive correlation values confirm that, for the values under analysis, there is a tendency to observe increasing wells flow rate classes, to the extent that higher-class ordinal values for the explanatory variables are observed, according to explained in Table 1 of Section 2.

As shown in Table 3, for the case of the dependent variable relate to well flow rate, the highest positive correlation is resulting from the lithology independent variable predominant (r = 0.274). This r value is similar to that obtained by Madrucci, Taioli and De Araújo (2008) in a study also performed on fractured aquifers in Brazil, when there was an r = 0.21. Likewise, it was identified that the dependent variable well flow rate class demonstrate a strong negative correlation with the distance to the billing location (rô = -0,484).

Table 3. Spearman correlation values obtained. ** Correlation is significant at level 0.01 (2-tailed). * Correlation is significant at level 0.05 (2-tailed).

Variables	**Produção do poço**	**Lithology**	**Lineament density**	**Drainage density**	**Distance from candidate drilling point to nearest lineament**
wells flow rate class	-	0,274**	0,212*	0,228*	-0,484**
Lithology	0,274**	-	-0,150	0,247**	0,013
Lineament density	0,212*	-0,150	-	0,120	0,216*
Drainage density	0,228*	0,247**	0,120	-	0,309**
Distance from candidate drilling point to nearest lineament	-0,484**	0,013	0,216*	0,309**	-

Figures 5, 6 and 7 show the cumulative distributions of the 113 wells flow rates, according to lithology, lineament and drainage classes, respectively. Figure 3 shows that although the lithology classified as very unfavorable is predominant for dry wells, it was also registered for the well with the highest flow rate. This aspect is justified by the fact that the well is located in a location that presents a classification of lineament density and very good and moderate drainage, respectively (Figures 6 and 7).

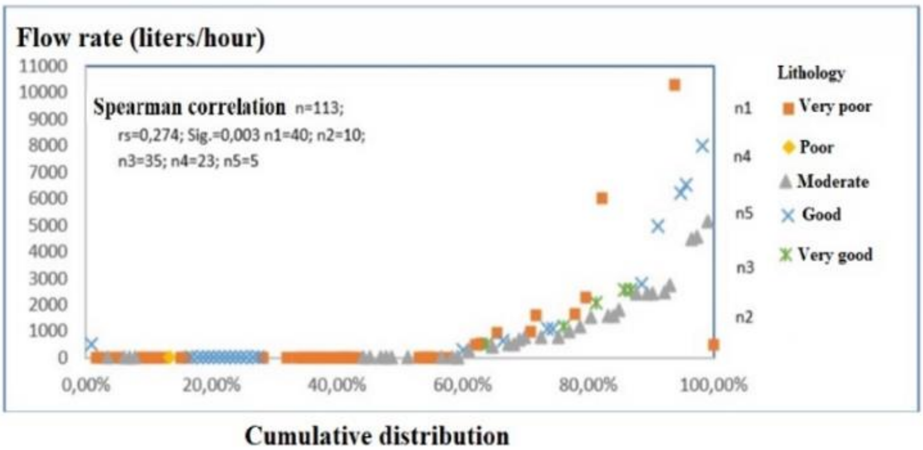

Figure 5. Cumulative distributions of the 113 wells flow rates relative to lithology.

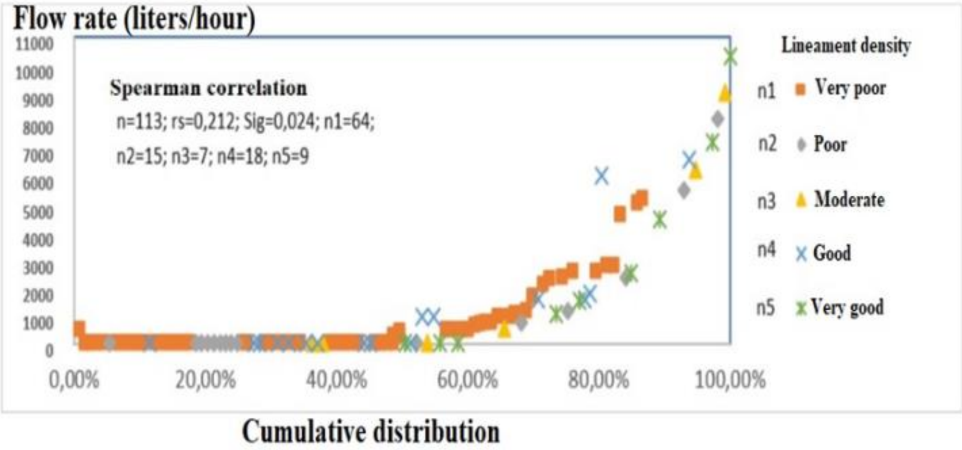

Figure 6. Cumulative distributions of the 113 wells flow rates relative to density of lineaments.

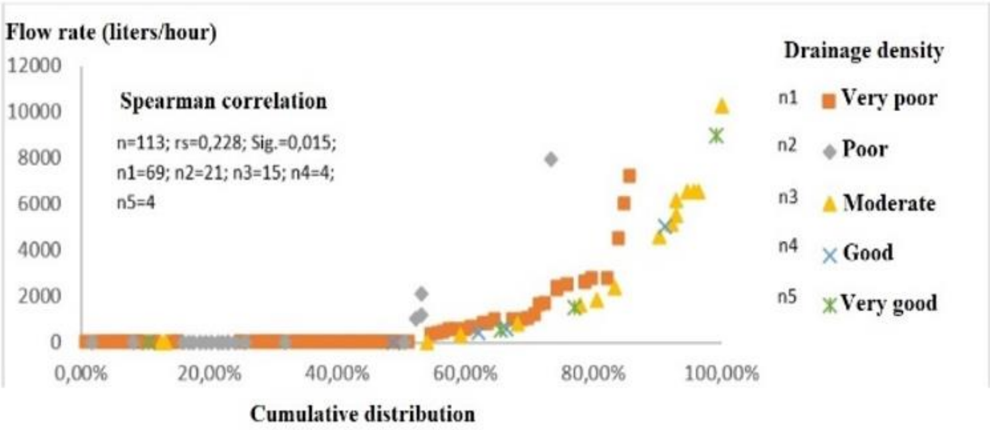

Figure 7 Cumulative distributions of the 113 wells flow rates relative to drainage density.

The identification of the relevant explanatory variables, shown in Table 3, allowed us to establish a predictive model of groundwater occurrence by a binomial logistic regression. Thus, assigning the value 0 (zero) to wells with flows rates below 1m³ / h and the value 1 (one) to wells with flows rates above 1 m³ / h, we obtained Equation 3, as following:

$$\hat{p} = \left(\frac{e^{-5,943+0,853*\mathrm{lit}+0,537*\mathrm{lin}+0.101*\mathrm{dren}+2,739*\mathrm{dist}}}{1+e^{-5,943+0,853*\mathrm{lit}+0,537*\mathrm{lin}+0.101*\mathrm{dren}+2,739*\mathrm{dist}}}\right) \quad (3)$$

wherein: flow rate class= $\begin{cases} 1, \text{se } \hat{p} \geq 50\% \\ 0, \text{se } \hat{p} < 50\% \end{cases}$

Equation 3 contains as independent variables the predominant lithology (lit), surface drainage (dren) and lineament density (lin) and distance from the candidate point to the nearest structural lineament identified (dist). The Nagelkerke R square indices obtained was 0.49, so that the model is able of explaining about

50% of the variations recorded in the dependent variable, ie, well production.

The validation of the obtained model was based on additional investigations discussed in Section 2, by drilling 43 additional wells, located along Folha Sousa 24-Z-B-A (Figure 8), encompassing the states of Ceará and Paraíba. The results obtained by applying Equation 3, and presented in Table 3, indicate that the prediction model established was able to correctly identify 25 of the 31 class 0 wells, corresponding to a 76% accuracy percentage, as well as correctly identified. 9 out of 12 wells with flow rates greater than $1m^3/s$ (75% accuracy), with an overall performance of 79.07%.

Figure 8. Groundwater favorability map.

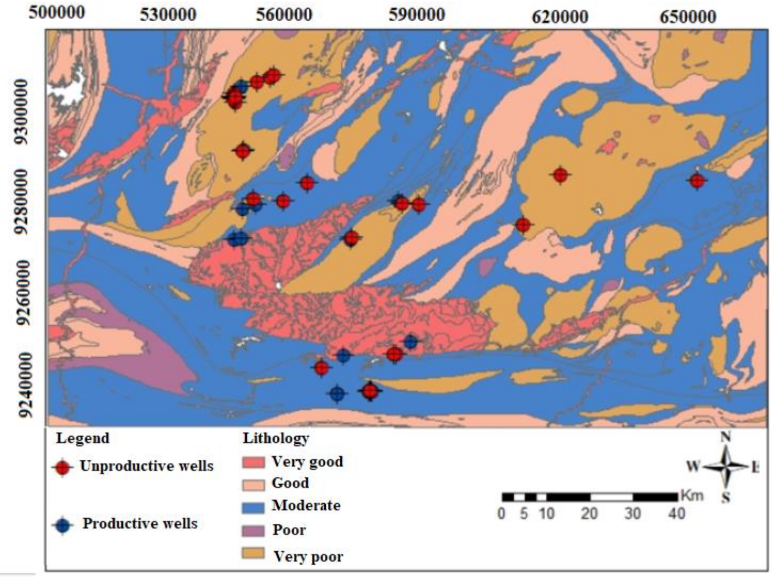

Table 3- Results

Predicted		Observed		Correct percentage
< $1m^3/h$	> $1m^3/h$	< $1m^3/h$	> $1m^3/h$	
25	6	31	12	76,0%
3	9			75,0%
Overall percentage				79,07%

Still, in Figure 8, it is possible to identify the predominance of unproductive wells in regions with lithologies classified as unfavorable, as well as a higher occurrence of productive wells in lithologies identified as quite favorable. The regions of moderate lithology show an alternation between productive and unproductive wells, increasing so the importance of the complementary analysis of the other independent variables of the model.

The investigations carried out were additionally accompanied by electrical resistivity tests, using DD arrangement according to the procedures presented in Section 2, aiming to identify in subsurface the adequacy of the geoprocessing results, as well as to verify the locations most susceptible to perforation of the wells. Figure 11 presents the example of one of the grid of electrodes executed in the field, for the municipality of Bernardino Batista-PB. In this locality, the interpretations of the images considered the predominant lithotypes of the study region, highlighted in Medeiros et al. (2005) by the presence of two well-characterized areas: the first described as Itaporanga Intrusive Suite, with the presence of porphyritic granites, granodiorites and quartz monzogranites (NP3_gamma_2it), and the second one including the Jaguaretama complex, with the local predominance of granitic to granodioritic orthogneiss. gray, migmatized (PP2j).

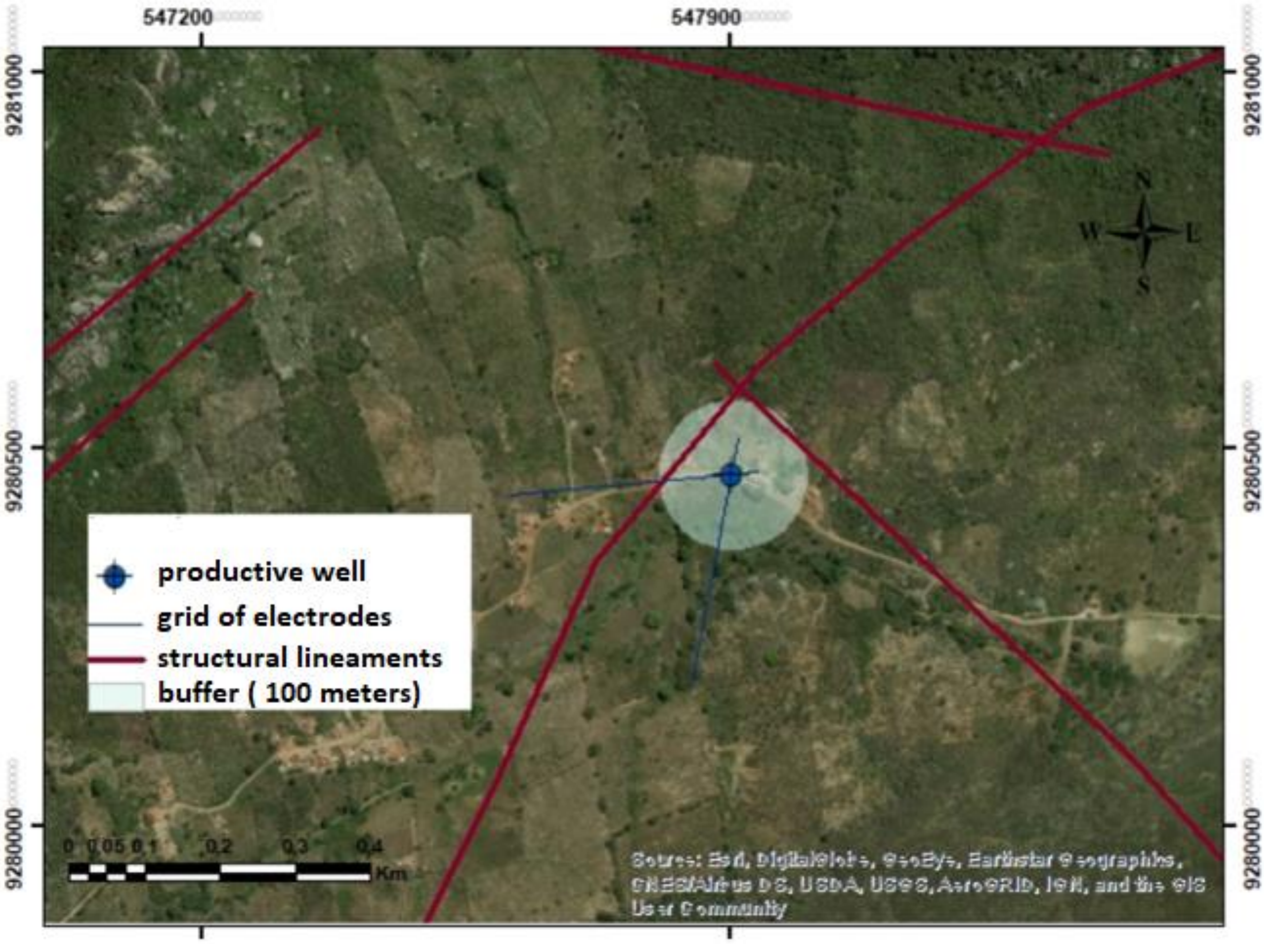

Figure 11. Geological context and DD arrangements in the municipality of Bernardino Batista.

Figures 12 and 13 show the Inversion models of the electric resistivity pseudo-sections obtained from the RES2DINV software for Line A and Line B, respectively. Given the geological location and the interpretation of the geoprocessing products, some specific points of the DD arrangement have been associated with likely fractures and / or regions where a top of unaltered rock deepens, and are represented in the images by blue and green colors, having lower resistivity values, ranging from 6 Ω.m. to 300 Ω.m. Areas with high resistivity values (reddish-yellow colors in the figures) were associated with possible occurrences of granitic / gneissic rocks and little or no alteration sites (low degree of fracture), ranging from 325 Ω.m to over 13000 Ω.m. Those same apparent resistivity variations occurred laterally between 32 and 88 meters of Line A and between 32m and 52 meters of Line B, whose interpretation of the cross profiles (Figure 14), allowed to confirm such variations in more than one direction. Considering the presence of strong structural lineaments in the region that are supposed to cross the geoelectric profiles, it was interpreted the presence of fracturing of the underlying rocks. Because of this, the well location was settled and drilled in the position represented by the orange arrow in the image of the apparent B-line electric resistivity section, thus 52 meters from the beginning of this linear section.

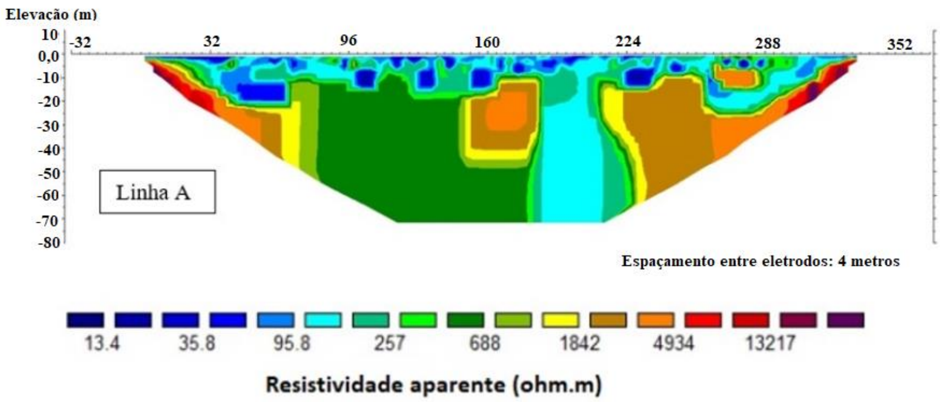

Figure 12. Pseudo-2D model of electric resistivity, (A-line) - Bernardino Batistaz

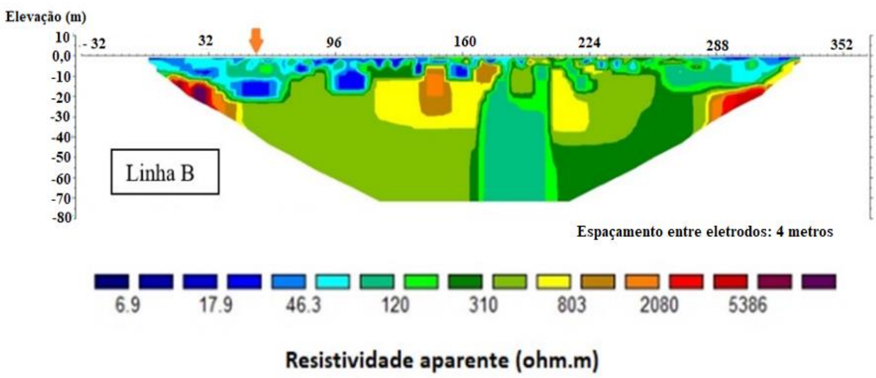

Figure 13. Pseudo-2D model of electric resistivity (B-line) - Bernardino Batista

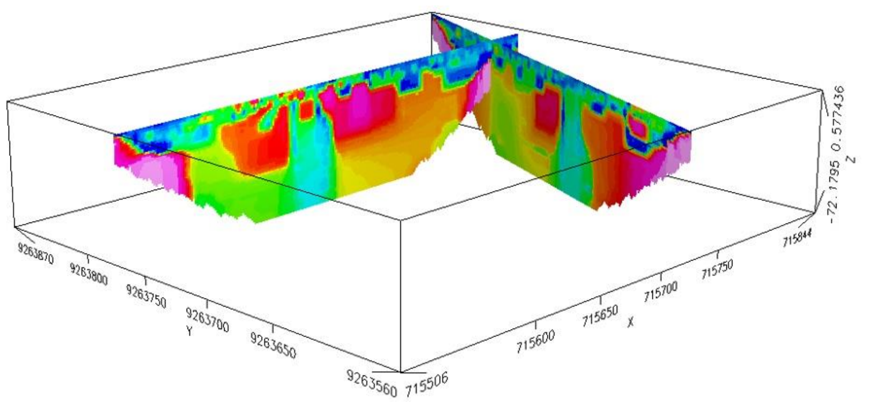

Figure 14. Cross-sections of electric resistivity - Bernardino Batista

5. Conclusions

The GIS techniques adopted in this research allowed the analysis of different predictors factors of groundwater occurrence (lineaments, lithology, drainage, and slope), correlating them with productivity data from wells drilled by the Brazilian Army in the northeastern semiarid. It was concluded that the variation in the productivity class of the drilled wells is influenced by the decision variables predominant lithotype, drainage density and density of structural lineaments and its distances up the candidate points to well drilling.

Moreover, a prospective hydrogeological model was developed in this study, and was be able to incorporate independent variables that presented statistical correlations consistent with previous studies conducted in other fractured-bedrock aquifer regions in Brazil. This model, which is based on logistic regression, proved effective in defining target areas for well drilling in the context of communities served by Operation Pipa Car, reducing the risk of setting unsuccessful wells locations. Such aspect reflects directly in the government costs involved in the prospecting activities, as well as in the social gains provided by the construction of productive wells near communities that need water.

However, during the validation of the model, it has also been verified productive wells in areas that the model indicated as unfavorable, as well as unproductive wells in locations evaluated as promising, thus revealing the complexity of the theme. It is common in the fractured domain of the Brazilian semiarid the occurrence of productive wells located nearby completely dry ones, and this could be attenuated, as evidenced in this paper, through the geophysical investigations performed. Therefore, it is recommended the development of future research in the search for modeling that will allow us to evaluate success rates in water well site location.

6. Acknowledgement

The research is financed by Brazilian Army and the CPRM (Geological Service of Brazil) for technical sup-port. This manuscript was considerably improved through comments and suggestions of two anonymous referees and the editors.

7. References

Bao, R., & Chen, J. (2022). Characteristics and problems of unplugged computer science curriculum for young children: Comparative and practical research based on the curriculum in four countries. *International Journal for Innovation Education and Research*, *10*(4), 1–22. https://doi.org/10.31686/ijier.vol10.iss4.3700

Cristo, H. S. de, Filho, A. S. N., Marinho de Aragão, J. W., & Saba, H. (2022). Media Bios and Artificial Intelligence: The dark side of Fake News. *International Journal for Innovation Education and Research*, *10*(4), 23–33. https://doi.org/10.31686/ijier.vol10.iss4.3701

Abuzied, S. M., Alrefaee, H. A. (2017). Mapping of groundwater prospective zones integrating remote sensing, geographic information systems and geophysical techniques in El-Qaà Plain area, Egypt. *Hydrogeology Journal*, *25, 2067-2088.*

Abuzied, S. M.; Ibrahim, S. K.; Kaiser, M. F.; Seleem, T. A. (2016). Application of remote sensing and spatial data integrations for mapping porphyry copper zones in Nuweiba area, Egypt. *International Journal of Signal Processing Systems, 4 (2), 102–108*.

Adetoyinbo, A. A.; Adelegan, F. T.; Bello, A. K. (2015) Environmental impact assessment of the potability of water from bore-hole, hand dug well and stream at Itagunmodi gold deposits Southwestern, Nigeria using FORTRAN algorithm for monitoring leachates and interpreting physicochemical data of contaminants in groundwater. *International Journal of Water Sources and Environmental Engineering, 7 (1), 1–6.*

Aziz, N. A.; Hasan, R. H.; Abdulrazzaq, Z. T. (2018). Optimum Site Selection for Groundwater wells using Integration between GIS and Hydrogeophysical Data. *Engineering and Technology Journal, v. 36, Part A, 6, p. 596-602*.

Binley, A.; Hubbard, S. S.; Huisman, J. A.; Revil A.; Robinson, D. A.; Singha, K.; Slater, L. D. (2015). The emergence of hydrogeophysics for improved understanding of subsurface processes over multiple scales. *Water Resources Research, 51, 3837–3866.*

Brandão, R. L.; Gomes, F. E. M. (2003). Técnicas de geoprocessamento e sensoriamento remoto aplicadas na avaliação de potencial hidrogeológico da Folha Irauçuba. *Revista de Geologia, 16 (1)*.

Conceição, R. A. C.; Silva, A. Q. (2013). Extração automática de lineamentos utilizando imagens SRTM, Landsat ETM+ e ALOS PALSAR na região de Nobres, MT. *In: XVI SIMPÓSIO BRASILEIRO DE SENSORIAMENTO REMOTO– SBSR, Foz do Iguaçu, PR.*

Cunha, A. P.; Marchezini, V.; Lindoso, D.; Saito, S.; Alvará, R. C. (2019). The challenges of Consolidation of a Drought-Related Disaster Risk Warning System to Brazil. *Sustentabilidade em Debate,10, 43-76.*

Das, S. Delineation of groundwater potential zone in hard rock terrain in Gangajalghati block, Bankura district, India using remote sensing and GIS techniques. (2017). *Modeling Earth Systems and Environment, 3 (4), 1589–1599.*

Elis, V. R.; Bondioli, A.; Ustra, A. T.; Carlos, I. M.; Pozzo, H. Â. P. D. (2019). Resistivity imaging for identification of fracture zones in crystalline bedrock in Brazil. *Sustainable Water Resources Management, 5 (3), 1089–1101.*

Hao, Z.; Hao, F.; Singh, V. P.; Ouyang, W.; Cheng, H. (2017). An integrated package for drought monitoring, prediction and analysis to aid drought modeling and assessment. *Environmental Modelling and Software, 91, 199-209.*

EMBRAPA (Brasil). (1979). Serviço Nacional de Levantamento e Conservação de Solos. In: REUNIÃO TÉCNICA DE LEVANTAMENTO DE SOLOS, 10., 1979, Rio de Janeiro. Súmula. Rio de Janeiro: EMBRAPA.

ESRI GIS and Mapping Software. Disponível em: http://www.esri.com/ . Acesso em: 12 abr 2022.

EXÉRCITO BRASILEIRO. Disponível em: https: //www. eb.mil.br/web/noticias/noticiario-doexercito/-/asset_publisher/ MjaG93KcunQI/content/operação semiarido-exercito-perfura-pocos-no-nordeste. Acesso em: 20 dez 2018.

Feitosa, Fernando A. C. (2008). Hidrogeologia: conceitos e aplicações/organização e coordenação científica. 3ª. ed. Rio de Janeiro: CPRM: LABHID,2008. 812 p.

Gallas, J. D. F.; Giardin, A. (2016). Eletrorresistividade na prospecção de aquíferos fraturados. *Águas subterrrâneas, 30(1), 119-138.*

Gonçalves, V. G.; Giampá, C. E. Q. Águas subterrâneas e poços tubulares profundos. (2009). *Engenharia Sanitaria e Ambiental*, v. 14, 3, IV-IV.

Gupta, R. P. (2003). Remote Sensing Geology, 2ªed., Springer, Springer-Verlag Berlin, Heidelberg, Germany, 665 p.

INPE. Disponível em: www.webmapit.com.br/inpe/topo data /. Acesso em: 17 mar 2022.

Keary, P.; Brooks, M.; Hill, I. Geofísica de Exploração. Editora Oficina de Textos, 438 p., 2009.

NASA. Disponível em: www2.jpl.nasa.gov/srtm/. Acesso em: 12 mar 2019.

Madrucci, V.; Taioli, F., De Araújo, C.C. (2008) Groundwater favorability map using GIS multicriteria data analysis on crystalline terrain, Sao Paulo state, Brazil. *Journal of Hydrology, 357, 3, 153–173.*

Martorana, R.; Capizzi, P.; D'alessandro, A.; Luzio, D. (2017). Comparison of different sets of array 245 configurations for multichannel 2D ERT acquisition. Journal of Applied Geophysics, v. 137, p. 34 – 48, 2017.

Medeiros, V. C.; Amaral, C. A.; Rocha, D. E. G. A.; Santos, R. B. (2005). PROGRAMA GEOLOGIA DO BRASIL - PGB. SOUSA. FOLHA SB.24-Z-A. ESTADOS DA PARAÍBA, RIO GRANDE DO NORTE E CEARÁ. Mapa Geológico. Recife: CPRM, 1 mapa, color., 66cm x 108cm. Escala 1:250.000.

Mohamaden, M. I. I.; El-Sayed, H. M.; Mansour, S. A. (2017). Combined application of electrical resistivity and GIS for groundwater exploration and subsurface mapping at northeast Qattara Depression, Western Desert, Egypt. Egyptian *Journal of Basic and Applied Sciences, 4 (1), 80–88*.

Nag, S. (2016). Delineation of Groundwater Potential Zones in Hard Rock Terrain in Kashipur Block, Purulia District, West Bengal, using Geospatial Techniques. *International Journal of Waste Resources, 6*.

Nam, W. H.; Hayes, M.J.; Svoboda, M.D.; Tadesse, T.; Wilhite, D. A. (2015). Drought hazard assessment in the context of climate change for South Korea. *Agricultural Water Management, 160, 106-117.*

Nazaruddin, D. A.; Amiruzan, Z. S.; Hussin, H.; Jafar, M. T. M. (2017). Integrated geological and multi-electrode resistivity surveys for groundwater investigation in Kampung Rahmat village and its vicinity, Jeli district, Kelantan, Malaysia. *Journal of Applied Geophysics, 138, 23–32.*

Ortega-Gaucin, D.; López Pérez M.; Arreguín, C. F. I. (2016). Drought Risk Management in Mexico: Progress and Challenges. *International Journal of Safety and Security Engineering , 6 (2), 161-170.*

Oldenburg, D.W.; Li, Y. (1999). Estimating depth of investigation in DC resistivity and IP surveys. *Geophysics, 64, 2, p. 403-416.*

Redhaounia, B.; Bedir, M.; Gabtni, H.; Ilondo, B.; Dhaoui, M.; Chabaane, A.; Khomsi, S. (2016). Hydro-geophysical characterization for groundwater resources potential of fractured limestone reservoirs in Amdoun Monts (North-western Tunisia). *Journal of Applied Geophysics, 128, 150–162.*

Silva, M. A; Moreira, C. A.; Borssatto, K., Ilha, L. M.; Santos, S. F. (2018). Geophysical prospection in tin mineral occurrence associated to greisen in granite São Sepé (RS). *REM - International Engineering Journal, 71, n. 2, 183-189.*

Sa, H. S.; Elis, V. R. (2016). Aplicação de imageamento elétrico multi-eletrodos para auxílio na locação de perfuração de poços tubulares: estudo de casos em aquíferos fraturados. *In: XIX CONGRESSO BRASILEIRO DE ÁGUAS SUBTERRÂNEAS, Campinas, p 2-11.*

Silva, C. D. A.; Rodrigues, R.S.; Lisoa, L.H.D. Locações de poços em ambiente cristalino: da análise estrutural aos dados de eletroresistividade. estudo de caso nos municípios de São Gonçalo do Amarante e Aratuba, Ceará. Anais do xx congresso brasileiro de águas subterrâneas, Campinas, 2018.

Silva, M. B.; Maia, R. B. (2017). Caracterização Morfoestrutural do Alto Curso da Bacia Hidrográfica do Rio Jaguaribe, Ceará-Brasil. *Revista Brasileira de Geomorfologia, 18, 3.*

Singh, K. K. K., Bharti, A. K.; PAL, S. K.; Prakash, A.; Saurabh, K. R.; Singh, P. K. (2019). Delineation of fracture zone for groundwater using combined inversion technique. *Environmental Earth Sciences, 78 (4), 110.*

Sivaramakrishnan, J.; Asokan, A.; Sooryanarayana, K. R.; Hegde, S. S.; Benjamin, J. (2015). Occurrence of Ground Water in Hard Rock Under Distinct Geological Setup. *Aquatic Procedia, 4, 706–712.*

Zar, J. (1999). Biostatistical analysis. 4. Ed. Upper Saddle River – New Jersey: Prentice Hall, 663 p.